ACS OMEGA

http://pubs.acs.org/journal/acsodf

Article

Pearlescent Mica-Doped Alginate as a Stable, Vibrant Medium for Two-Dimensional and Three-Dimensional Art

Anne M. Arnold,* Zachary C. Kennedy, Joshua A. Silverstein, Jacob F. Ellis, and Janine R. Hutchison

Cite This: *ACS Omega* 2021, 6, 18694−18701

Read Online

ACCESS | Metrics & More | Article Recommendations | Supporting Information

ABSTRACT: Emergent technologies are driving forces in the development of innovative art media that progress the field of modern art. Recently, artists have capitalized on the versatility of a new technology to create, restore, and modify art: additive manufacturing or three-dimensional (3D) printing. Additively manufactured art relies heavily on plastic-based materials, which typically require high heat to induce melting for workability. The necessity for heat limits plastic media to dedicated 3D printers. In contrast, biologically derived polymers such as polysaccharides used to create "bioinks" often do not require heating the material for workability, broadening the types of techniques available for printing. Here, we detail the formulation of a bioink consisting of mica pigments suspended in alginate as a new, vibrant art medium for 2D and 3D compositions. The properties that make alginate an ideal colorant binder are detailed: low cost with wide availability, nontoxicity and biocompatibility, minimal color, and an array of attractive physicochemical properties that offer workability and processing into 2D and 3D structures. Further, the chemical composition, morphology, and dispersibility of an array of mica pigment additives are characterized in detail as they pertain to the quality of an art medium. Alginate-based media with eight mica colors were formulated, where mica addition resulted in vibrantly colored inks with moderate hiding power and coverage of substrates necessary for 2D printing with thin horizontal and vertical lines. The utility of the media is demonstrated via the generation of 2D and 3D vibrant structures.

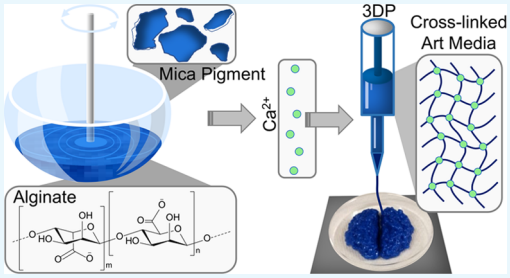

1. INTRODUCTION

Artistic compositions such as paintings, sculptures, and reliefs exploit diverse types of media. Traditional media include oil paint, acrylic paint, stone, wood, charcoal, wax, and clays.[1] Important criteria for the selection and application of these traditional media are first, the ability to work or process them effectively but furthermore their ability to confer color and texture to the finished composition. The power of color as a design element is well-studied given its ability to create unconscious responses and illicit physical reactions from observers. As stated previously, "the right color can make or break a work of art or design."[2] To this end, art media that allow for rich and diverse expression of color have been adapted throughout history. Pigments or dyes with vast chemical compositions are used to produce striking colors with desirable effects and are derived typically from natural or synthetic minerals or organic molecules.[3−6] A liquid or a malleable solid with a wide variation in viscosity or consistency is typically used to bind or disperse the colorants in the media. The resulting colorant-integrated formulations make up the media used to produce 2D and 3D compositions.

In contrast to traditional art media, new art media (e.g., digital art, computer animation, etc.) utilized by artists to create contemporary compositions are driven by the advent of innovative technologies. An exciting technology to foster creation of new types of artworks is additive manufacturing or 3D printing (3DP). The suite of 3DP technologies popularized in recent decades has had a significant impact on the art community. 3DP has been adopted in the art world in areas such as cinema, theater, music, visual arts, dance, and art education.[7] In dance, 3D scanning and 3DP technology have been utilized in a unique way to create customizable ballet shoes, known as the P-ROUETTE, to mediate the pain and damage to the feet of dancers.[8] 3DP has also been integrated into art education,[9−12] where traditional 2D paintings can be converted into embossed or 2.5 dimensional pieces to enhance the educational experience for the visually impaired.[11]

Development and focus on the use of 3DP for the arts have been based primarily on the use of synthetic, petrochemical-derived, polymer (e.g., thermoplastic) feedstocks.[13] The integration of colorants such as dyes and pigments[14] or phosphors[15] into thermoplastics, for example, is well-established given the ubiquity of plastic usage in the world. These thermoplastic feedstocks often necessitate processing with heat or UV light and, therefore, can require dedicated printing hardware to operate.[16,17] In contrast, biologically

Received: March 17, 2021
Accepted: June 11, 2021
Published: July 14, 2021

Table 1. Criteria Considered when Selecting Alginate as the Binding Medium Used in This Study

Similar physicochemical properties compared to a commercial binding medium	Xanthan gum is used as a binding medium in commercial acrylic products, suggesting that alginate, which has similar physicochemical properties, could also serve as a successful binding medium
Tunable cross-linking	Alginate cross-linking can be achieved rapidly at room temperature using calcium chloride in a tunable fashion for optimal workability
Minimal color	Reduces color dampening of pigments
Moderate opacity	Opacity of the binding medium promotes substrate coverage
Optimal consistency, workability, and stiffness	Eight percent (w/v) alginate solutions have optimal consistency to suspend pigments up to 8 days and are stiff enough to retain a 3D form but are not too thick to hinder workability
Low cost	≤$0.10 USD/g (as of February 2021)
Wide availability	Available for purchase from industrial and retail suppliers
Water dispersibility at neutral pH	At neutral pH values, water is a biologically and environmentally friendly solvent, eliminating hazards associated with other solvent systems
Nontoxicity and biocompatibility	Alginate serves as an essential food additive and is used in pharmaceutical and biomedical products

derived polymers such as carbohydrates used to create bioinks—3D printable hydrogel matrices—often do not require heating the material for 3DP.[18,19]

The use of bioinks and biologically derived polymers, in general, for 3DP is widespread;[18] however, little attention has been given to using these materials as 3D printable artistic media. The most frequently encountered, naturally occurring organic materials in art and art conservation have been summarized in detail elsewhere.[20,21] Notably, biologically derived polymers, such as animal glues derived from collagen connective tissues and egg- and casein-derived mixtures of proteins, have been employed as binding media in paintings, specifically tempera. Moreover, polysaccharide natural gums from trees are of significance as medium components for watercolors.[20] In contemporary art media, xanthan gum, another biologically derived polymer, is used as a binder and thickening agent in acrylic emulsion paints.[22] Xanthan gum is commonly used in other commercial products to increase the viscosity of a formulation and aid in the suspension of solid particles.[23] An alternative cheap, widely used bioink for 3DP is alginic acid or alginate salt that is sourced and refined from brown seaweeds on an industrial scale.[24] Alginate is a polysaccharide copolymer[19,25] with high molecular weight (10−100 kDa typically) that, like xanthan, turns into a viscous gum when hydrated and a robust hydrogel when cross-linked with cations, such as Ca^{2+}.[19,25] Inspired by the similarity of the physicochemical properties of alginate and xanthan gum and the growing body of knowledge of alginate as a bioink for 3DP, we hypothesized that alginate could serve as a colorant binder (or a binding medium) and have utility as a new art medium with high processability.

Here, we detail the formulation of mica-doped alginate as a new, vibrant art medium for 2D and 3D compositions. The physical properties and utility of using alginate as a pigment binder are introduced. The chemical composition, morphology, and dispersibility of an array of mica pigments are characterized in detail as these properties affect the quality of the resulting media: color, hiding power or opacity (ability to cover a substrate), and pearlescence (pearl-like luster appearance).[26−28] Additionally, the medium quality was evaluated with respect to the tinctorial strength (capacity of a pigment to impart color to a medium) and hiding power using colorimetry and ultraviolet−visible (UV−vis) absorption spectroscopy, respectively. The utility of the mica-loaded alginate media is demonstrated via the generation of vibrant, 2D and 3D structures.

2. RESULTS AND DISCUSSION

2.1. Alginate as a 3D Printable Binding Medium.

Alginate was chosen as a printable binding medium capable of dispersing colorant particles due to a host of desirable properties, as outlined in Table 1. Initial interest in alginate stemmed from the similarity of alginate's physicochemical properties to xanthan gum, which is a commercially available binding medium used in acrylic paints. The benefit of alginate, when compared to other gum-forming polysaccharides, is the capacity to form cross-links to transform the pseudostable structures into stable gels that retain a 3D shape. These desirable cross-linking properties are a result of alginate's chemical structure. That is, the backbone structure of alginate consists of blocks of (1,4)-linked β-D-mannuronate (M) and α-L-guluronate (G) residues, as depicted in Figure 1. The anionic G residues are those that participate in cross-linking by chelating cations (most commonly Ca^{2+}) between polymer chains, which enable formation of hydrogels.[29,30]

The physicochemical properties of alginate inks and hydrogels, such as color and opacity, create an optimal binding medium for pigment dispersion and 3D printability (Table 1). When hydrated, alginate lacks color (Figure S1), a desirable

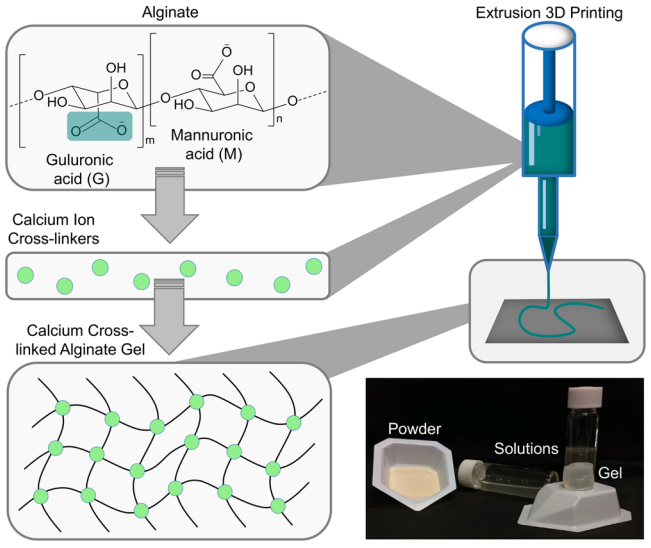

Figure 1. Depiction of the chemical structure, cross-linking, and extrusion 3DP capability of alginate as well as a photo depicting the alginate powder, 8% (w/v) solutions, and the calcium cross-linked gel. Note that the G subunit carboxylates, highlighted in green, in the polysaccharide backbone participate in the ionic cross-linking with calcium ions to form gels.

https://doi.org/10.1021/acsomega.1c01453
ACS Omega 2021, 6, 18694−18701

trait so as not to dampen the color of added pigments, and is semiopaque to provide substrate coverage. Alginate forms a viscous gum that offers the perfect balance between pigment dispersion and workability and stiffness to form pseudostable 3D structures.

Additionally, alginate is well-suited as a colorant binder as it is low-cost, widely available, water-dispersible in neutral conditions, and nontoxic and biocompatible (Table 1). The cost of alginate when procured on a small scale (5 kg) from a scientific supplier in the United States is $0.10 USD/g (as of February 2021), and it is readily available for retail consumers and industry at similar or even lower costs. Harsh solvents are not required to disperse alginate; in fact, alginate is dispersible in water at neutral pH. Alginate is also nontoxic and biocompatible, serving as an essential food additive in numerous consumer products[31] such as ice cream,[24,32−34] beer,[24] and edible food packaging[35] and a main component in pharmaceutical and biomedical products.[36]

Thus, in this work, we utilized a sodium alginate solution prepared by dissolution into water to achieve a final alginate concentration of 8% weight to volume (w/v). However, additional polymer systems that meet the criteria outlined in Table 1 could also be used as a suitable binding medium, creating an exciting opportunity for future work. Of practical importance, it is notable that the aqueous alginate formulation may be premade and stored at room temperature for on-demand use as desired. Alginate solutions stored for longer than 1 month did not result in any noticeable performance decreases compared to freshly prepared solutions or observable microbial overgrowth despite being unsterilized.

2.2. Mica Pigment Dispersibility in a 3D Printable Binding Medium. Chemical composition, particle morphology, and dispersibility of mica pigments affect the color, hiding power, and pearlescence in a multifaceted interplay (Figure S2). In this study, we selected mica pigments of eight different colors (Figure 2 and Figure S3a) with intermediate hiding power and high pearlescence. A more detailed discussion of mica pigment physicochemical characterizations is provided in the Supporting Information (Sections S1 and S1.1−S1.4, Figures S2−S8, and Tables S1−S10).

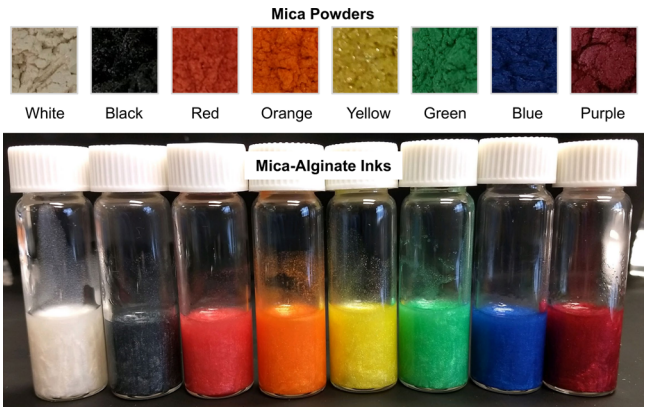

Figure 2. Visual representation of mica powders and mica-alginate inks used for 3D printing.

Pigment dispersibility in a colorant binder is perhaps one of the most pertinent characteristics that impact art medium quality. Poor pigment dispersibility and stability of pigment dispersions over time create undesirable heterogeneous color, hiding power,[37] and pearlescent effects.[38] Thus, choosing an appropriate pigment and binding medium combination that imparts superior pigment dispersion and stability is essential. Since mica pigments are advertised as water-dispersible, we hypothesized that our aqueous-based alginate solutions may be a suitable dispersing agent. Here, we compared the dispersibility of mica pigments in water and 8% (w/v) alginate solutions as a function of time. Interestingly, we observed that some mica colorants at a 1% w/v loading did not disperse completely in water (Figure S3f), whereas all mica pigments completely dispersed in alginate solutions (Figure 2 and Figure S3f). Over the course of the settling experiment, mica colorants significantly settled out of water within 24 h, while alginate solutions retained complete pigment dispersibility (Figures S3f and S9). In fact, the alginate binding medium was so successful that mica pigments remained dispersed up to 8 days until visual settling was observed. After settling, the mica-loaded alginate inks were easily redispersed with mechanical agitation (similar to mixing/shaking/inverting of bottles of paint before use), demonstrating shelf-life stability (Figure S9).

2.3. Properties of Mica-Doped Alginate Media.

2.3.1. Color of Alginate-Based Mica Media. Pigments that have a high tinctorial strength are more desirable as colorants for art media. High tinctorial pigments generally create media with brighter colors using a smaller pigment to binding medium ratio as compared to low tinctorial pigments. With respect to the resulting media, color dictates the medium value, where a vibrant medium is preferred because it has a larger range of accessible colors through mixing.

Here, we evaluated the color of the eight mica pigment powders and the tinctorial strength of pigments when dispersed and gelled in the alginate binding medium using 3D colorimetry. 3D colorimetry is an objective approach to quantify color using a 3D coordinate system, which removes the subjectivity in describing colors that may be perceived differently across individuals. Specifically, we utilized the CIELAB color space system ($L^*a^*b^*$) that classifies colors using three criteria (i.e., coordinates) including lightness (L^*, relative brightness), hue (a^*, color or shade), and saturation (b^*, color intensity).[39]

The L^*, a^*, and b^* color values for the mica pigments and mica-loaded alginate gels are reported in Figure 3, in addition to the RGB values represented as color swatches. We found that, in most of the cases, there were small differences in color between pure mica pigments and the mica-loaded alginate gels, as demonstrated by the low ΔE2000 color difference values. This suggests that mica pigments had a high tinctorial strength. White and orange mica pigments had the highest tinctorial strength with ΔE2000 values of 1.72, indicating that color differences between pigments and gels could only be perceived with close observation. The remaining mica colors had lower tinctorial strengths, where color differences could be perceived at a glance (ΔE2000, 2−10). Interestingly, purple mica powder, which was the only iron-coated pigment, had the lowest tinctorial strength with a ΔE2000 value of 8.88.

2.3.2. Hiding Power (Opacity) of Mica-Alginate Gels. We predicted, based on the physicochemical properties of the mica pigments and the alginate binding medium, that our art media would have moderate hiding power (opacity). To probe the extent of opacity as a function of gel thickness, we utilized ultraviolet−visible (UV−vis) absorption spectroscopy (Figure 4 and Figure S10). We found that addition of mica pigments increased the optical density (i.e., opacity) of the gels when

https://doi.org/10.1021/acsomega.1c01453
ACS Omega 2021, 6, 18694−18701

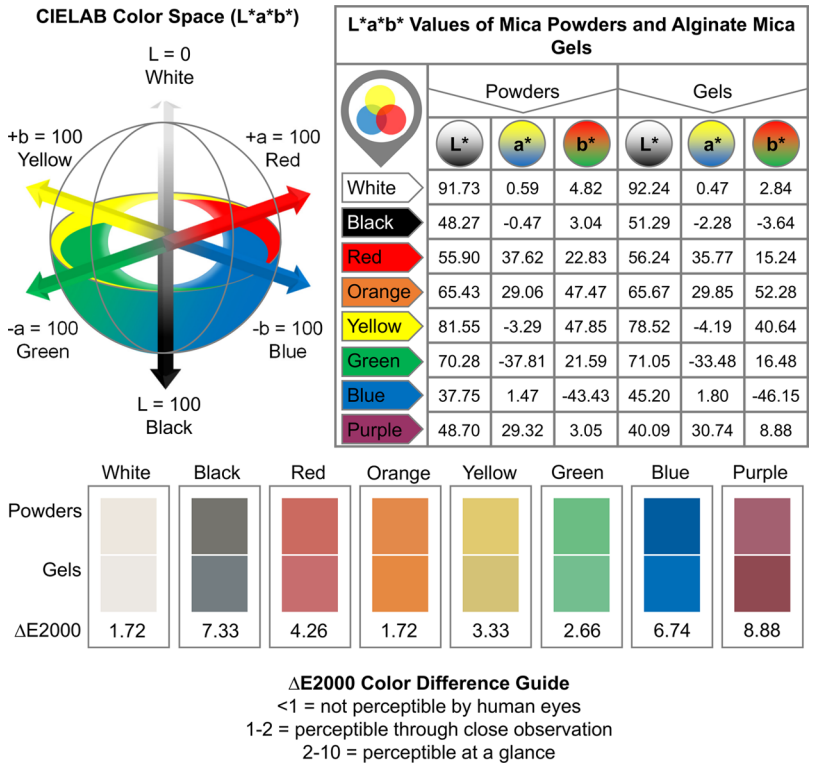

Figure 3. Representation of the CIELAB color space ($L^*a^*b^*$) coordinate system and the L^*, a^*, and b^* values of the mica pigment powders and calcium cross-linked alginate gels with a 1% (w/v) mica loading. Note that the gels also had an 8% (w/v) loading of alginate. The L^*, a^*, and b^* color measurements of the powders and gels were converted into RGB values and represented as color swatches. The corresponding ΔE2000 color difference between the pure mica powders and mica-loaded alginate gels is displayed below the color swatches.

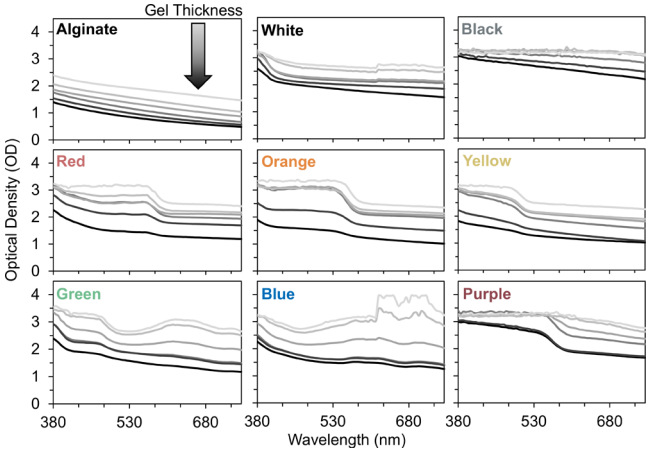

Figure 4. Ultraviolet−visible (UV−vis) absorption spectroscopy of pure alginate and 1% (w/v) mica-loaded alginate gels as a function of gel thickness. Note that the gels contain an 8% (w/v) loading of alginate and were cross-linked via calcium exposure.

compared to pure alginate gels. Qualitatively, we also observed that even at small thicknesses, the mica-loaded alginate gels had moderate opacity, which is especially relevant for 2D art that uses thin, horizontal and vertical lines.

2.4. 2D and 3D Printing Capability of the Mica-Alginate Media. The consistency of our mica-alginate media can be readily tuned based on the artist's needs for a particular piece of art. The media, if used as is, have thinner consistency that readily flows, which may be desirable for some art techniques (e.g., approaches similar to paint pouring or traditional painting). However, the consistency necessary for creating other types of art, such as the 2D and 3D printing that we address, requires thicker media. Thicker media can be attained, and tuned, by adding calcium chloride to the medium preprint, which creates media that are partially cross-linked and more readily retain their shape during the printing process. We found that less viscous media were optimal for 2D printing, while thicker media were necessary for 3DP to retain the shape of the print (Figure 5). In all cases, addition of an excess of calcium chloride after the completion of the print can still be used to completely cross-link the piece for maximum stability.

Alginate-based 3D prints are stable over a period of several weeks if they are preserved at room temperature in a neutral, 200 mM calcium chloride solution. The preservation solution prevents the prints from desiccating, where desiccation results in shape distortions, shrinkage, and cracking of the 3D constructs. The calcium chloride solution maintains the shape and size of 3D prints and eliminates print cracking. During storage, mica pigments remain dispersed in the print and maintain their pearlescence and color, which is a result of the chemical,[40] thermal,[40,41] and photostability of mica pigments.[40]

Our current storage method of alginate-based 3D constructs is intended for short-term preservation; thus, our alginate-based 3D prints are not archival using calcium chloride storage. In fact, alginate is a biodegradable polymer,[31] a property that we find desirable in a binding medium. The biodegradability of alginate prevents excess waste accumulation if the constructs are discarded, unlike plastic, 3D printed constructs that take years to centuries to degrade.[42] Increasing shelf-life stability of 3D printed constructs, if desired, could be explored in future work. That is, shelf-life stability could be accomplished by investigating alternative storage approaches, such as resin

https://doi.org/10.1021/acsomega.1c01453
ACS Omega 2021, 6, 18694−18701

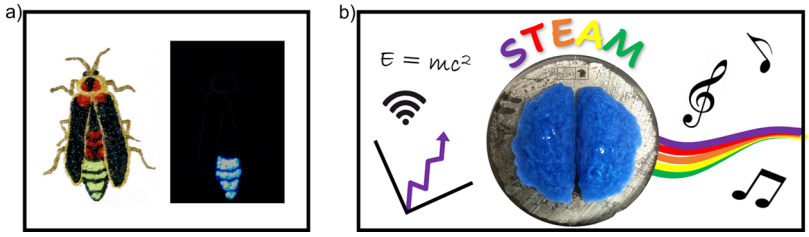

Figure 5. Demonstration of the utility of mica-loaded alginate bioinks to produce 2D and 3D structures. (a) 3D printed, 2D art of a firefly, using a glow-in-the-dark additive to depict the luminescent abdominal region of the firefly lantern. (b) 3D printed, 3D structure depicting the anatomy of a brain stored in 200 mM calcium chloride.

casting. Additionally, polymers that are less susceptible to degradation could be utilized as the ink binding medium.

3. CONCLUSIONS

Here, we thoroughly characterized the physicochemical properties of eight mica colorants with respect to chemical composition, morphology, and dispersibility in the colorant binder, as these properties affect the color, hiding power, and pearlescence of art media. We concluded that the physicochemical properties of mica colorants were optimized to provide vibrant color, moderate hiding power, and maximum pearlescence. We also detailed the compatibility of mica colorants with alginate as a binding medium, where alginate served as a superior mica dispersant compared to water and provided shelf-stable dispersions that could be prepared in advance for later use. Our bioinks were vibrantly colored with moderate hiding power while also demonstrating their utility to print 2D and 3D structures by tuning the consistency of the ink based on the needs of the artist. Thus, we conclude that our new, mica-doped alginate bioinks can be utilized as effective media to produce diverse forms of art.

4. MATERIALS AND METHODS

4.1. Chemical Reagents and Vendors. Sodium alginate (product no. W201502; manufacturer reported viscosity at 1% (w/v) in water at 25 °C of 5−40 cps) and anhydrous calcium chloride (product no. C1016; ≤7.0 mm granular) were purchased from Sigma-Aldrich. Mica pigment powders (Muerk, 50 color set epoxy resin dye powdered pigments) were purchased from Amazon LLC. Eight mica powder pigment colors were used for all experiments. It is of note that the manufacturer pigment color names used were shinny white, black, red, orange, shinny yellow, bright green, cobalt, and purple, which are referred to in this work as white, black, red, orange, yellow, green, blue, and purple, respectively.

4.2. Material Preparations. *4.2.1. Sodium Alginate Solutions.* Sodium alginate solutions (8% w/v in deionized water) were prepared by addition of deionized water (400 mL) to sodium alginate (32 g). To promote sodium alginate dissolution, solutions were vigorously stirred at room temperature until alginate was completely dissolved (1−3 days). The mica-loaded sodium alginate solutions were prepared by adding 1% (w/v) mica pigment to an 8% sodium alginate solution (i.e., 150 mg of mica per 15 mL of alginate) followed by manual stirring until the colorant was homogeneously dispersed.

4.2.2. Calcium Gelation of 8% (w/v) Sodium Alginate. Gelation of 8% (w/v) sodium alginate solutions for colorimetry and ultraviolet−visible absorption spectroscopy was induced by adding a 1:1 volume ratio of 200 mM calcium chloride to alginate solutions (including pure alginate and 1% (w/v) mica-loaded alginate) to create rectangular-shaped, bulk gels with thicknesses of >10 mm. Samples were then sealed to prevent evaporation and allowed to equilibrate overnight at room temperature before testing.

4.2.3. Preparation of 8% (w/v) Sodium Alginate Gels for Ultraviolet−Visible Absorption Spectroscopy. A #6 disposable tissue biopsy punch was used to acquire cylinders/disks from thick, rectangular, bulk gels. A scalpel was used to cut the alginate cylinders into thinner disks for analysis. A total of six different thicknesses for each gel were used for ultraviolet−visible absorption spectroscopy. The thicknesses of the gel disks were measured with calipers. The average thickness and standard deviation for all gels at each thickness interval are reported in Table 2.

Table 2. Thickness of Gels Measured by Ultraviolet−Visible Absorption Spectroscopy

average (mm)	0.73	1.03	1.53	1.85	2.16	3.53
standard deviation (mm)	0.03	0.03	0.05	0.09	0.09	0.08

4.2.4. Bioink Formulation for 2D and 3D Printing. For the glow-in-the-dark ink used for 2D printed art, Glo Gel (Glo Germ) was added to 1% (w/v) mica-loaded sodium alginate solutions (containing 8% (w/v) alginate) in a 1:5 v/v ratio (i.e., 2 mL of Glo Gel for every 10 mL of ink). Then, alginate inks were semicross-linked using 200 mM $CaCl_2$. To semicross-link for 2D printing, 200 mM $CaCl_2$ was added in a 1:10 v/v ratio to mica-loaded alginate solutions (i.e., 1 mL of 200 mM $CaCl_2$ for every 10 mL of alginate solution). For 3DP inks, 200 mM $CaCl_2$ was added in a 1:5 v/v ratio to mica-loaded alginate solutions (i.e., 1 mL of 200 mM $CaCl_2$ for every 5 mL of alginate solution). In the case of all ink preparations, $CaCl_2$ was added slowly (∼5 drops at a time) followed by rigorous mechanical stirring with a metal spatula. Once all $CaCl_2$ was added, the bioink was loaded into a polypropylene syringe (from the top by removing the plunger) and forced through the syringe aperture into a 50 mL Falcon tube to create a homogeneous ink devoid of clumps. The Falcon tube was then centrifuged for 5 min at 10,000*g* using an Eppendorf centrifuge 5810 R (15 Amp version) to remove air bubbles from the ink.

4.3. Material Characterization. *4.3.1. Optical Images and Microscopy.* Optical images of powders, solutions, and gels were acquired using a 16 megapixel camera. With respect to optical microscopy, mica pigment powder samples were prepared by drop casting 10 μg mL^{-1} solutions dispersed in deionized water onto microscope slides. A coverslip was added after water evaporated from the samples. The samples were then imaged on an inverted, Labomed MET 4000 microscope

https://doi.org/10.1021/acsomega.1c01453
ACS Omega 2021, 6, 18694−18701

using a 40× Infinity LWD Phase Plan objective lens (N.A., 0.6) and Micron version 2.0.0 software.

4.3.2. Scanning Electron Microscopy (SEM) with Energy-Dispersive X-ray spectroscopy (EDS). Scanning electron microscopy and energy-dispersive X-ray spectroscopy were performed using a JEOL JSM-7001F-field emission gun (FEG) scanning electron microscope (SEM) with a Bruker xFlash 6|60 EDS spectrometer. Backscatter electron (BSE) imaging and EDS analysis were performed at an accelerating voltage of 15 kV and a probe current setting at 10 (2 nA). EDS analysis was performed using Bruker Esprit 2.0 software.

4.3.3. Fourier Transform Infrared (FTIR) Spectroscopy. FTIR spectroscopy of mica powder pigments was performed on a Bruker Tensor II FT-IR spectrometer with an A225/Q Platinum attenuated total reflectance (ATR) attachment furnished with a diamond crystal. The background and sample spectra were an average of 64 scans, where raw spectra were collected in absorbance over a range of 4000−400 cm^{-1} with a 4 cm^{-1} resolution. A background scan was performed for each sample analyzed. An ATR correction and automatic, rubber band baseline correction were performed on raw spectra using OPUS 7.5 software. Then, all spectra were normalized to an absorbance of 0.2 using the Si−O peak (∼995 cm^{-1}).

4.3.4. Particle Size Analysis. The pigment particle size distributions were measured by laser diffraction using a Horiba LA-960 particle size analyzer. A blank was recorded in pure deionized water prior to each sample measurement. Dry pigment powder (∼10−15 mg) was added directly into the 150 mL reservoir, and the resulting suspension was mechanically agitated in the cell while in circulation mode to disperse the particles. Measurements were then recorded with a circulation setting of 3 and agitation turned off. For size calculations, refractive indices of 1.590 and 1.333 were used for mica and water, respectively. The particle size distributions are plotted by volume percentage (q).

4.3.5. 2D Particle Shape Analysis. Particle shape analysis was conducted using the microscopy images of mica pigment powders as described above. The microscopy images were processed in ImageJ (National Institutes of Health, Bethesda, Maryland), where RGB images were converted to 8-bit then to a binary image type. Finally, the binary images were subjected to the fill holes function followed by the outline processing features (see Figure S6).

The particle morphology of six particles for each mica pigment color was analyzed in ImageJ, with care taken to identify single particles for analysis while excluding aggregates. The 2D shape descriptors used to analyze mica particles include the roughness (R_o), aspect ratio (AR), radius sphericity (S_r), and roundness (R) (see Figure S8). The R_o of particles was ascertained using the "ConvexitySolidarity" macro provided by ImageJ that measured the perimeter (P) and convex perimeter (C_{PER}) of each particle. R_o was then determined using eq 1.[43]

$$R_o = \frac{C_{PER}}{P} \tag{1}$$

The AR was calculated by measuring the minimum and maximum Feret lengths, which are x_{Fmin} and x_{Fmax}, respectively, in ImageJ using the "Analyze Particles" function. Particle AR was calculated using eq 2.[43]

$$AR = \frac{x_{Fmin}}{x_{Fmax}} \tag{2}$$

S_r of particles were determined manually by fitting a minimum circumscribing circle, where the radius is $r_{min\text{-}cir}$, and a maximum inscribed circle, where the radius is $r_{max\text{-}in}$, to each particle. S_r was calculated using eq 3.[44]

$$S_r = \frac{r_{max-in}}{r_{min-cir}} \tag{3}$$

Lastly, R was also determined manually, where circles were fitted to the corners of particles. The radii of the circles are denoted as r_i, where i nomenclature refers to the number of the corner in which the circle is fitted (arbitrarily assigned during analysis). R was calculated numerically using the following equation[44]

$$R = \frac{\sum \left(\frac{r_i}{r_{max-in}} \right)}{N_i} \tag{4}$$

where N_i is the number of corners.

4.3.6. Settling Experiment. Mica powder dispersions in deionized water and mica-loaded alginate solutions, both with a 1% w/v loading, were prepared in glass vials. Optical images of the samples were acquired directly after mixing samples and referred to as "as-mixed." The samples were imaged 24 h after the initial mixing to document the degree of particle settling in the samples. The time frame for the settling experiment for alginate dispersions was extended due to minimal settling after 24 h. Mica-dispersed alginate solutions were imaged again after 8 days when particle settling began to become obvious followed by images of solutions after manual redispersion of mica pigments in alginate.

4.3.7. Colorimetry. A handheld PCE-CSM 2 colorimeter (PCE Instruments) was used to record the color of the pigment powders and the bulk, pigment-doped gels as described above. The color was recorded in the CIE $L^*a^*b^*$ color space. Two measurements were performed on each sample, and the values for each of the L^*, a^*, and b^* values were averaged. The surface color change from that of pure pigment powder to pigment-doped gels was quantified using the ΔE2000 method,[45] which ranges from 0 (colors are exactly the same) to 100 (colors are the exact opposite).

4.3.8. Ultraviolet−Visible (UV−Vis) Absorption Spectroscopy. All UV−vis absorption spectra were acquired on a Tecan Safire plate reader using Magellan 7.2 sp1 software and a clear, polystyrene, flat-bottom 96-well tissue culture plate. Data was acquired in absorbance measurement mode using a wavelength scan acquired over 300−800 nm and a 5 nm step size. Further, data was acquired at room temperature using a COS96fb plate definition file with no plate lid. Each well had 50 reads with 10 ms in between movements and reads.

Mica pigment powders were analyzed using 100 $\mu g\ mL^{-1}$ dispersions in deionized water. Each measurement was made by adding a 300 μL dispersion to the 96-well plate and immediately acquiring the UV−vis absorption spectra to prevent particle sedimentation. All spectra of the mica pigment powder dispersions were baseline-subtracted from deionized water.

Mica-loaded alginate gels with various thicknesses, where the preparation procedure is described above, were placed in a 96-well plate for analysis. All spectra of the mica-loaded alginate gels were baseline-subtracted from an empty well.

4.4. 2D and 3D Printing of Mica-Loaded Alginate Inks. The bioink formulations, which were prepared as

https://doi.org/10.1021/acsomega.1c01453
ACS Omega 2021, 6, 18694−18701

described above, were carefully loaded into a 10 mL polypropylene syringe (from the top by removing the plunger) to prevent inclusion of bubbles into the ink. Then, an 18 gauge blunt-tipped needle was added to the syringe for printing. Both 2D and 3D prints were conducted by hand at room temperature onto either a glass or plastic surface, respectively, and subsequently imaged.

■ ASSOCIATED CONTENT

Supporting Information

The Supporting Information is available free of charge at https://pubs.acs.org/doi/10.1021/acsomega.1c01453.

> Additional discussion of particle size distributions, morphology, and morphology distributions of mica pigment particles; colorimetry of a calcium cross-linked alginate gel (Figure S1); effect of mica properties on art medium quality (Figure S2); measured physicochemical properties of mica (Figure S3); Fourier transform infrared spectroscopy of mica pigments (Figure S4 and Table S1); particle size distributions of mica colorants (Figure S5 and Table S2); image processing procedure of optical microscopy images of mica particles (Figure S6); scanning electron microscopy images of mica particles (Figure S7); representation of particle morphology analysis of mica pigments (Figure S8); results of particle morphology analysis of mica pigments (Tables S3−S10); prolonged settling experiment of mica pigments dispersed in alginate (Figure S9); ultraviolet−visible absorption spectroscopy of water-dispersed mica colorants (Figure S10) (PDF)

■ AUTHOR INFORMATION

Corresponding Author

Anne M. Arnold − *Chemical and Biological Signatures Group, National Security Directorate, Pacific Northwest National Laboratory, Richland, Washington 99354, United States;* orcid.org/0000-0001-8743-4685; Email: anne.arnold@pnnl.gov

Authors

Zachary C. Kennedy − *Chemical and Biological Signatures Group, National Security Directorate, Pacific Northwest National Laboratory, Richland, Washington 99354, United States;* orcid.org/0000-0003-2479-8232

Joshua A. Silverstein − *Material Development and Testing Group, Energy and Environment Directorate, Pacific Northwest National Laboratory, Richland, Washington 99354, United States*

Jacob F. Ellis − *Controls Optimization and Network Group, Energy and Environment Directorate, Pacific Northwest National Laboratory, Richland, Washington 99354, United States*

Janine R. Hutchison − *Chemical and Biological Signatures Group, National Security Directorate, Pacific Northwest National Laboratory, Richland, Washington 99354, United States*

Complete contact information is available at: https://pubs.acs.org/10.1021/acsomega.1c01453

Notes

The authors declare the following competing financial interest(s): Pacific Northwest National Laboratory has filed a provisional patent on behalf of the authors.

■ ACKNOWLEDGMENTS

This work was supported by the Lab Directed Research and Development (LDRD) Program at the Pacific Northwest National Laboratory (PNNL), a laboratory operated by Battelle for the U.S. Department of Energy under contract DE-AC05-76RLO 1830.

■ REFERENCES

(1) Mavrody, S. *Visual Art Forms: Traditional to Digital*; Belisso: 2013.

(2) Bleicher, S. *Contemporary Color Theory and Use*; 2nd ed.; Cengage Learning: 2011.

(3) Falcón, T. D. *The Encyclopedia of Archaeological Sciences*; American Cancer Society: 2018; pp. 1−3, DOI: 10.10.1002/9781119188230.saseas0203.

(4) Yusuf, M. *Handbook of Renewable Materials for Coloration and Finishing*; John Wiley & Sons: 2018, DOI: 10.1002/9781119407850.

(5) Finney, B. *The History of Art in Color*; http://chrysler.org/the-history-of-art-in-color-modern/ (accessed Feb 11, 2021).

(6) Dawson, T. L. Examination, Conservation and Restoration of Painted Art. *Color. Technol.* **2007**, *123*, 281−292.

(7) ALL3DP *3D Printed Art: How 3D Printing Makes Its Way into Creativity*. https://all3dp.com/2/3d-printed-art-how-3d-printing-makes-way-into-creativity/ (accessed Feb 13, 2021).

(8) *Hadar Neeman*. https://2018.bezalel.ac.il/en/industrial-design/hadar-neeman/ (accessed Feb 13, 2021).

(9) Menano, L.; Fidalgo, P.; Santos, I. M.; Thormann, J. Integration of 3D Printing in Art Education: A Multidisciplinary Approach. *Comput. Sch.* **2019**, *36*, 222−236.

(10) Sweeny, R. W. Making and Breaking in an Art Education Makerspace. *J. Innovation Entrepreneurship* **2017**, *6*, 9.

(11) Chen, Y.; Chang, P. 3D Printing Assisted in Art Education: Study on the Effectiveness of Visually Impaired Students in Space Learning. In *2018 IEEE International Conference on Applied System Invention (ICASI)*; IEEE: 2018; pp. 803−806. DOI: 10.10.1109/ICASI.2018.8394384.

(12) Kwon, Y. M.; Lee, Y.-A.; Kim, S. J. Case Study on 3D Printing Education in Fashion Design Coursework. *Fash. Text.* **2017**, *4*, 26.

(13) Rea, A. Art, Printed: Computers Are Redefining Fine Art. But Is That a Good Thing?. In *Growler Magazine*; MIT Press: 2019.

(14) Muller, B. 24b - Colorants for Thermoplastic Polymers. In *Applied Plastics Engineering Handbook*; Kutz, M. Ed.; Plastics Design Library; William Andrew Publishing: Oxford, 2011; pp. 435−440. DOI: 10.10.1016/B978-1-4377-3514-7.10043-1.

(15) Zhou, L.; Hong, J.; Li, X.; Shi, J.; Tanner, P. A.; Wong, K.-L.; Wu, M. Bright Green Emitting $CaYAlO_4$:Tb^{3+},Ce^{3+} Phosphor: Energy Transfer and 3D-Printing Artwork. *Adv. Opt. Mater.* **2020**, *8*, 2000523.

(16) Ngo, T. D.; Kashani, A.; Imbalzano, G.; Nguyen, K. T. Q.; Hui, D. Additive Manufacturing (3D Printing): A Review of Materials, Methods, Applications and Challenges. *Composites, Part B* **2018**, *143*, 172−196.

(17) Prabhakar, M. M.; Saravanan, A. K.; Lenin, A. H.; leno, I. J.; Mayandi, K.; Ramalingam, P. S. A Short Review on 3D Printing Methods, Process Parameters and Materials. *Mater. Today Proc.* **2020**, *45*, 6108.

(18) Gungor-Ozkerim, P. S.; Inci, I.; Zhang, Y. S.; Khademhosseini, A.; Dokmeci, M. R. Bioinks for 3D Bioprinting: An Overview. *Biomater. Sci.* **2018**, *6*, 915−946.

(19) Hospodiuk, M.; Dey, M.; Sosnoski, D.; Ozbolat, I. T. The Bioink: A Comprehensive Review on Bioprintable Materials. *Biotechnol. Adv.* **2017**, *35*, 217−239.

(20) Doménech-Carbó, M. T. Novel Analytical Methods for Characterising Binding Media and Protective Coatings in Artworks. *Anal. Chim. Acta* **2008**, *621*, 109−139.
(21) National Academy of Sciences *Scientific Examination of Art: Modern Techniques in Conservation and Analysis*; The National Academies Press: Washington, DC, 2005. DOI: 10.10.17226/11413.
(22) Jablonski, E.; Learner, T.; Hayes, J.; Golden, M. Conservation Concerns for Acrylic Emulsion Paints. *Stud. Conserv.* **2003**, *48*, 3−12.
(23) Katzbauer, B. Properties and Applications of Xanthan Gum. *Polym. Degrad. Stab.* **1998**, *59*, 81−84.
(24) Sabra, W.; Zeng, A.-P.; Deckwer, W.-D. Bacterial Alginate: Physiology, Product Quality and Process Aspects. *Appl. Microbiol. Biotechnol.* **2001**, *56*, 315−325.
(25) Axpe, E.; Oyen, M. L. Applications of Alginate-Based Bioinks in 3D Bioprinting. *Int. J. Mol. Sci.* **2016**, *17*, 1976.
(26) Gueli, A. M.; Bonfiglio, G.; Pasquale, S.; Troja, S. O. Effect of Particle Size on Pigments Colour. *Color Res. Appl.* **2017**, *42*, 236−243.
(27) BYK Additives & Instruments *Wetting and Dispersing Additives*; BYK Additives & Instruments.
(28) Rohrer, A.; Venturini, M. T. *Pearlescent Pigments in Coatings − a Primer*. https://www.pcimag.com/articles/105225-pearlescent-pigments-in-coatings-a-primer?v=preview (accessed Jan 20, 2021).
(29) Lee, K. Y.; Mooney, D. J. Alginate: Properties and Biomedical Applications. *Prog. Polym. Sci.* **2012**, *37*, 106−126.
(30) Shah, P. P.; Shah, H. B.; Maniar, K. K.; Özel, T. Extrusion-Based 3D Bioprinting of Alginate-Based Tissue Constructs. *Procedia CIRP* **2020**, *95*, 143−148.
(31) Martău, G. A.; Mihai, M.; Vodnar, D. C. The Use of Chitosan, Alginate, and Pectin in the Biomedical and Food Sector—Biocompatibility, Bioadhesiveness, and Biodegradability. *Polymer* **2019**, *11*, 1837.
(32) Bahramparvar, M.; Tehrani, M. M. Application and Functions of Stabilizers in Ice Cream. *Food Rev. Int.* **2011**, *27*, 389−407.
(33) Clarke, C. *The Science of Ice Cream*; Royal Society of Chemistry: 2015.
(34) Homayouni, A.; Javadi, M.; Ansari, F.; Pourjafar, H.; Jafarzadeh, M.; Barzegar, A. Advanced Methods in Ice Cream Analysis: A Review. *Food Anal. Methods* **2018**, *11*, 3224−3234.
(35) Senturk Parreidt, T.; Müller, K.; Schmid, M. Alginate-Based Edible Films and Coatings for Food Packaging Applications. *Foods* **2018**, *7*, 170.
(36) Batista, P. S. P.; de Morais, A. M. M. B.; Pintado, M. M. E.; de Morais, R. M. S. C. Alginate: Pharmaceutical and Medical Applications. In *Extracellular Sugar-Based Biopolymers Matrices*; Cohen, E., Merzendorfer, H. Eds.; Biologically-Inspired Systems; Springer International Publishing: Cham, 2019; pp. 649−691. DOI: 10.10.1007/978-3-030-12919-4_16.
(37) Hunger, K.; Schmidt, M. U. *Industrial Organic Pigments: Production, Crystal Structures, Properties, Applications*; John Wiley & Sons: 2019.
(38) Sekar, N. Optical Effect Pigments for Technical Textile Applications. In *Advances in the Dyeing and Finishing of Technical Textiles*; Gulrajani, M. L. Ed.; Woodhead Publishing Series in Textiles; Woodhead Publishing: 2013; pp. 37−46, DOI: 10.10.1533/9780857097613.1.37.
(39) *Defining and Communicating Color: The CIELAB System*; Sappi Fine Paper North America: 2013.
(40) Pan, X.-F.; Gao, H.-L.; Lu, Y.; Wu, C.-Y.; Wu, Y.-D.; Wang, X.-Y.; Pan, Z.-Q.; Dong, L.; Song, Y.-H.; Cong, H.-P.; Yu, S.-H. Transforming Ground Mica into High-Performance Biomimetic Polymeric Mica Film. *Nat. Commun.* **2018**, *9*, 2974.
(41) Hosseini Zori, M. Synthesis and Characterization of Red Pearlescent Pigments Based on muscovite and Zirconia-Nano-encapsulated Hematite. *Prog. Color, Color. Coat.* **2012**, *5*, 7−13.
(42) Chamas, A.; Moon, H.; Zheng, J.; Qiu, Y.; Tabassum, T.; Jang, J. H.; Abu-Omar, M.; Scott, S. L.; Suh, S. Degradation Rates of Plastics in the Environment. *ACS Sustainable Chem. Eng.* **2020**, *8*, 3494−3511.
(43) Olson, E. PARTICLE SHAPE FACTORS AND THEIR USE IN IMAGE ANALYSIS − PART 1: THEORY. *J. GXP Compliance* **2011**, *15*, 17.
(44) Rodriguez, J. M.; Edeskär, T.; Knutsson, S. Particle Shape Quantities and Measurement Techniques−A Review. *Electron. J. Geotech. Eng.* *18* , 169.
(45) Luo, M. R.; Cui, G.; Rigg, B. The Development of the CIE 2000 Colour-Difference Formula: CIEDE2000. *Color Res. Appl.* **2001**, *26*, 340−350.

https://doi.org/10.1021/acsomega.1c01453
ACS Omega 2021, 6, 18694−18701